# ASSESSMENT OF A TIME DEPENDENT DAMAGE ACCUMULATION MODEL FOR CRACK GROWTH AT HIGH TEMPERATURE

**A. F. LIU**
**Rockwell International**
**North American Aircraft Division**
**Los Angeles, California 90009**
**U. S. A.**

## ABSTRACT

This paper presents a perspective view on crack growth at high temperatures. A quantitative assessment on crack growth mechanisms under various combinations of stress, temperature, and time has been conducted. A crack growth accumulation model has been formulated (based on superposition principal) to compute crack growth rates under constant amplitude, constant frequency loading (i.e., no load interaction). The capability of the present model to handle the combined effects of stress amplitude, cyclic frequency, and dwell time is demonstrated. It is also shown that if the influence of sustained load on subsequent crack growth behavior can be quantitatively determined, the existing method for predicting room temperature spectrum load crack growth can be updated to formulate a generic, multi-functional methodology suitable to high temperature application.

## INTRODUCTION

Current fracture mechanics theory treats cyclic crack growth as a linear elastic phenomenon. Residual strength of a test coupon, or a structure, is frequently computed based on linear elastic fracture indexes. Elastic-plastic, or fully plastic analysis such as the J-integral approach is used when large scale yielding occurs. All the existing crack growth analysis methods for spectrum life prediction basically deal with using material constant amplitude crack growth rate data to compute crack growth history of a structural element. For crack growth at high temperature, the conventional crack growth methodology that was based on material room temperature behavior will no longer be applicable.

To understand the complex interaction mechanisms of stress, temperature, time, and environmental exposure, research effort has been directed at identifying high temperature crack growth mechanism in various engineering alloys. A vast amount of experimental and analytical data (available in the literature) was reviewed and analyzed to find out which fracture mechanics parameters are applicable to characterize material behavior at high temperature, and to determine the phenomenological factors that influence load/environment interaction mechanism. In order to enable micromechanical modeling to be made to account for the contribution of each variable to the total behavior of crack growth, these data were gathered into groups representing a variety of isolated loading events (which could be considered as simulations to aircraft in service conditions). Schematic representations of several typical loading profiles under consideration are shown in Figure 1. Actually, crack growth behavior for thirty-six types of loading profiles, which were in excess of sixty (60) combinations in material, temperature, frequency and time variations, were examined. The result of a qualitative evaluation of these variables was presented in a previous paper.[1] The present paper deals with a quantitative assessment of an approach for crack growth analysis needed for predicting damage tolerance of airframe structures in a high temperature environment.

## BASIC CONSIDERATIONS

The sketches in Figure 1 indicate that the current method for predicting crack growth life in an ambient environment (i.e., room temperature air, with the absence of corrosive media) deals with using the constant amplitude crack growth rate data to predict structural life under spectrum loads. There is a good reason to believe that cyclic frequency and the shape of a stress cycle play an insignificant role on either constant amplitude or spectrum crack growth behavior. The magnitude and sequential occurrences of the stress cycles are the only key variables affecting room temperature crack growth behavior. Therefore, an accurate representation of the material crack growth rate data as a function of the stress amplitude ratio (i.e., the so-called crack growth law or crack growth rate equation), and a load interaction model for monitoring the load sequence effects on crack growth (the commonly called crack growth

retardation/acceleration model), are the only two essential elements in today's crack growth life predictive methodology.

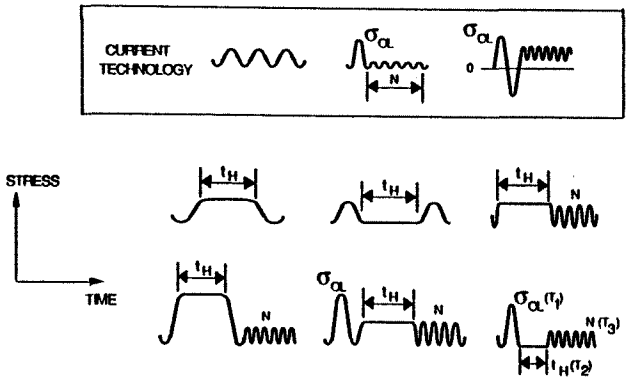


Fig. 1 Typical segments in an aircraft load spectrum

The basic concept for room temperature crack growth analysis can be adapted to formulate an updated method for predicting high temperature crack growth. However, significant modifications on characterization of material properties, and the load interaction and damage accumulation models are required. This is due, in part, to increasing numbers of variables involved in defining the elevated temperature crack growth behavior. Most important, the time factor in a given stress cycle (whether it is associated with hold time or low frequency), which promotes time dependent crack growth behavior, can no longer be ignored. Just for showing the complexity in high temperature crack growth, a comparison of all the major elements involved in room temperature and high temperature crack growth is presented in Table 1. Illustrations on how these elements should be integrated into an analytical methodology are given in the following sections.

Depending on material, temperature, time, and environment, crack growth at elevated temperature can exhibit various degrees of creep deformation at the crack tip region; thereby the crack tip characterizing parameter may vary from linear elastic K to time dependent $C_t$, then to the steady state creep parameter, $C^*$.[1]-[3] Consider that creep resistance of a material is characterized by the coefficient and exponent of the minimum creep rate to stress relationship, i.e.,

$$\dot{\varepsilon} = A \cdot S^n \qquad (1)$$

Thus the degree of creep deformation is a function of stress level and time at load. For a stress cycle of which the hold time is relatively short, the size of a creep zone will be relatively small (or non-existent for no hold time).

If a material is environment sensitive, it is usually resistant to creep deformation thereby its creep zone size will be smaller than those creep zones in the creep ductile materials. Upon reviewing and analyzing a vast amount of creep crack growth data (available in the literature), it was concluded that most aircraft high temperature superalloys belong to the creep resistant/environment sensitive category.[1] For all practical purposes, it is conceivable that the linear elastic index K can adequately characterize the high temperature crack growth behavior in these alloys. Therefore, in the reminder of this paper, discussions will be centered on cumulative damage modeling with K. It is shown that an advanced crack growth predictive methodology must include the fol-

**Table 1 Comparison of fracture mechanics elements for room temperature and high temperature crack growth**

| | Room Temperature | High Temperature |
|---|---|---|
| Dependent Variables: | da/dN | da/dN, da/dt, Mixed |
| Functions of: | R-ratio | R-ratio, Temperature, Frequency, Wave Form |
| Controlling Parameter: | K, J | K, $C_t$, $C^*$ |
| Crack Tip Deformation Mode: | Plasticity ($F_{ty}$, n) | Plasticity ($F_{ty}$, n)<br>Stress Relaxation due to Creep (E, A, n, t)<br>Environmental Diffusion Coefficients (Q, R, t) |
| Spectrum Life: | Single Mode for Load Interaction | Multiple Modes for Load/Temperature/Time Interactions |

lowing:

1. Three types of material characterization data, i.e., (a) the conventional, cycle dependent, da/dN data as functions of K (stress intensity level), R (cyclic stress ratio), and T (temperature), (b) the sustained load, time dependent, da/dt data as functions of K and T, and (c) the post sustained load da/dN data.

2. Methods that can account for load interaction including the effects of time (t) and temperature.

## CYCLE DEPENDENT VERSUS TIME DEPENDENT CRACK GROWTH

For most engineering alloys, the effect of frequency on constant amplitude crack growth rate is probably negligible in dry air environment. However, the crack growth rate varies significantly at elevated temperature and in chemically aggressive environments. Cyclic wave form, hold time, or the combination of these with temperature, or corrosive environment, further complicates the crack growth behavior of a given material. Experimental investigations regarding one or more of these variables have been carried out by many investigators. The bibliographies compiled in References (1) through (4) represent a good portion of the published documentation on this subject.

If cyclic crack growth testing at high temperature is done in a traditional way, i.e., in a sinusoidal (or symmetrically triangular) wave form at a moderately high frequency, the crack growth rates are functions of $\Delta K$ and R. Thus, the phenomenon is similar to those at room temperature with the following exceptions: (1) For a given R, the value of $\Delta K_{th}$ is higher at higher temperature. (2) For a given R, the terminal $\Delta K$ value is higher at higher temperature because $K_C$ is usually higher at a higher temperature due to the fact that $F_{ty}$ (i.e., the material tensile yield strength) is lower at a higher temperature.

A schematic representation of temperature influence on da/dN is shown in Figure 2. It should be noted that crack growth rates are not always higher at temperatures higher than room temperature as it is implied in Figure 2. Depending on frequency and $\Delta K$ range, some material (particularly those sensitive to environment) may exhibit slower crack growth rates at intermediate temperatures. Moisture, which might have acted like a corrosive media, was vaporized by heat, therefore the magnitude of the environmental fatigue component (which inherently associates with crack propagation) would be reduced.[5]

Cyclic frequency, or duration of a stress cycle (i.e., hold time), plays an important role in high temperature crack growth. At high frequency, i.e., fast loading rate with short hold time (or no hold time), the crack growth rate is cycle dependent, i.e., crack growth rate is represented by da/dN. At low frequency, or with long hold time, the crack growth rate is time dependent, i.e., da/dN is in proportion to the total time span of a given cycle. For the tests of different cycle times, all crack growth rate data points

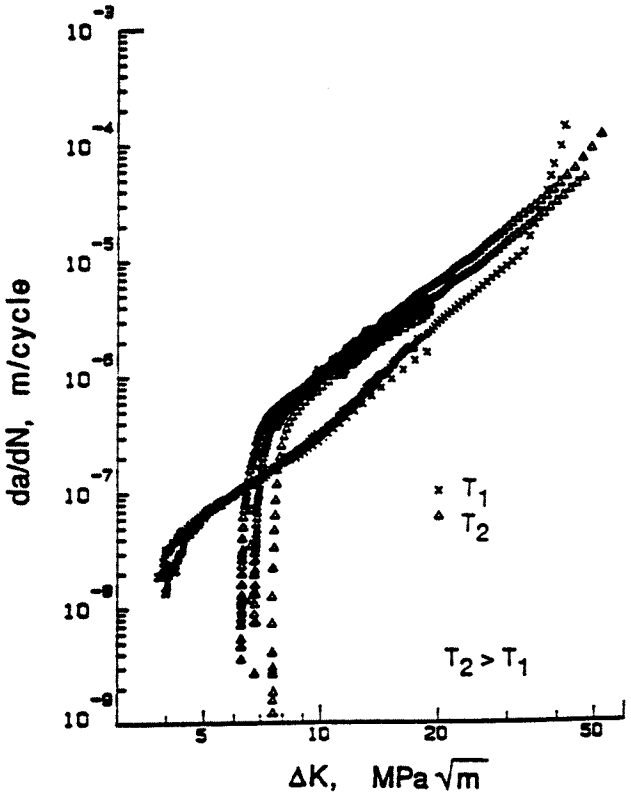


Fig 2 Schematic temperature influence on da/dN

are collapsed into a single curve of which da/dt is the dependent variable. A mixed region exists in between the two extremes. The transition from one type of behavior to another depends on material, temperature, frequency, and R. For a given material and temperature combination, the transition frequency is a function of R. The frequency range at which the crack growth rates remain being time dependent increases as R increases.[6] The limiting case is R approaches unity. It is equivalent to crack growth under sustained load, for which the crack growth rates at any frequency will be totally time dependent.

Research conducted on conventional high temperature super alloys, the INCO 718 in particular, have shown that sustained load creep crack growth rate data can be used to predict cyclic crack growth in the time dependent regime.[6]-[8] In those regions in which the cycle dependent and the time dependent phenomena are both present, implementation of a semi-empirical technique [9] may be required. An

elucidation on formulating a collective procedure to predict crack growth in the time dependent regime is given below:

Applying the Wei-Landes superposition principle for subcritical crack growth in aggressive environment,[10] crack growth rate for a given stress cycle can be treated as the sum of three parts: (1) the uploading part (i.e., the load rising portion of a cycle), (2) the hold time, and (3) the down loading (unloading) portion of a cycle. Therefore

$$\frac{da}{dN} = \left(\frac{da}{dN}\right)_r + \left(\frac{da}{dN}\right)_H + \left(\frac{da}{dN}\right)_d \qquad (2)$$

It has been shown frequently, by experimental tests, that the amount of da for the unloading part is negligible unless the stress profile is unsymmetric, and the uploading time to the unloading time ratio is significantly small, i.e., the unloading time (compared to the uploading time) is sufficiently long. For simplicity, we will limit our discussions to those cases based on two components only, i.e., by setting $(da/dN)_d$ equal to zero. However, the $(da/dN)_r$ term may be cycle dependent, or time dependent, or mixed. This term consists of two parts, i.e., one part accounts for the cyclic wave contribution and another part accounts for the time contribution. Consequently, Equation (2) can be rewritten as

$$\frac{da}{dN} = \left(\frac{da}{dN}\right)_c + \left(\frac{da}{dN}\right)_t + \left(\frac{da}{dN}\right)_H \qquad (3)$$

The first term on the right hand side of Equation (3) represents the cycle dependent part of the cycle. It comes from the conventional crack growth rate data at high frequency, i.e., it follows those "crack growth laws" cited in the literature. A comprehensive discussion in review of this subject is given in Reference 11. In reality, when a stress cycle is totally cycle dependent, the magnitude of the second term on the right hand side of Equation (3) will be negligibly small. On the other hand, when a stress cycle is totally time dependent, the contribution of $(da/dN)_c$ to the total da/dN is negligible; thereby the validity of Equation (3) in respect to full frequency range is maintained.

When a crack growth rate component exhibits time dependent behavior, it is equivalent to crack growth under a sustained load of which the crack growth rate description is defined by da/dt (instead of da/dN) as

$$\frac{da}{dt} = C \cdot (K_{max})^m \qquad (4)$$

This quantity is obtained from a sustained load test.

To express the second term on the right hand side of Equation (3) in terms of da/dt, consider a generalized function that can describe K at any given time in a valley to peak cycle. That is:

$$K(t) = R \cdot K_{max} + 2K_{max} \cdot (1-R) \cdot t_r \cdot f \qquad (5)$$

where $t_r$ is the time required for ascending the load from valley to peak, f is the frequency of the cyclic portion of a given load cycle. For symmetric loading $t_r = f/2$, Equation (5) gives $K(t) = K_{min}$ at $t_r = 0$, and $K(t) = K_{max}$ at $t_r = f^{-1}/2$. The amount of crack extension over a period $t_r$ can be obtained by replacing the $K_{max}$ term of Equation (4) by K(t), and integrating, i.e.,

$$\left(\frac{da}{dN}\right)_t = C \cdot \int_0^{t_r} [K(t)]^m \bullet dt \qquad (4a)$$

For any positive value of m, Equation (4a) yields

$$\left(\frac{da}{dN}\right)_t = C \cdot (K_{max})^m \cdot t_r \cdot R_m \qquad (6)$$

where

$$R_m = (1 - R^{m+1}) / [(m+1) \cdot (1 - R)] \qquad (7)$$

A parametric plot for $R_m$ as a function of R is shown in Figure 3. It is seen that $R_m$ increases as R increases.

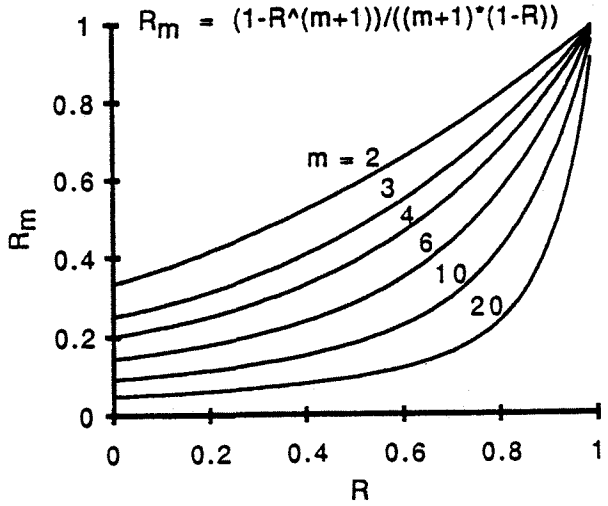


Fig 3 Parametric representation of $R_m$

Therefore, for a given $K_{max}$, $(da/dN)_f$ increases as R increases in the time dependent regime. This trend is in reverse to those customary observed in the high frequency, cycle dependent regime.

The third term on the right hand side of Equation (3) simply equals to da/dt times the time at sustained load. Recognizing that the first term on the right hand side of Equation (6) is actually equal to da/dt, finally, Equation (3) can be expressed as:

$$\frac{da}{dN} = \left(\frac{da}{dN}\right)_c + \frac{da}{dt} \cdot t_r \cdot R_m + \frac{da}{dt} \cdot t_H \qquad (8)$$

where $t_H$ is the hold time.

The applicability of Equation (8) is demonstrated in Figures 4 and 5. In these figures, the test data were generated from the INCO 718 alloy, at 649°C, having various combinations of ΔK, R, $t_H$, and f. The test data, which were extracted from the open literature,[7],[8] are presented in the figures along with the predictions.

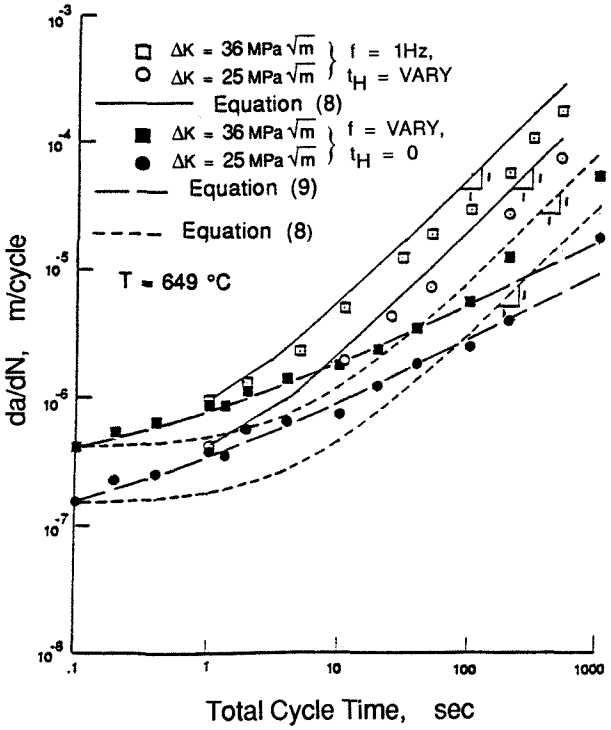


Fig 4 Comparison of predicted and test results for the INCO 718 alloy at R = 0.1

One of the two data sets in Figure 4 was generated using trapezoidal stress cycles of which f = 1Hz (i.e., 0.5 second for uploading, and 0.5 second for unloading) and $t_H$ = 1-500 sec. The data points for the other data set were obtained by conducting tests at various frequencies without hold time. A constant ΔK level, either 25 MPa $\sqrt{m}$ or 36 MPa $\sqrt{m}$ with R = 0.1, was applied to all the tests. Crack growth rate per cycle was plotted as a function of total time per cycle. For example, for a total cycle time of 100 second, it would mean that the test was conducted at a frequency of 1Hz with $t_H$ = 99 second, or f = 0.01Hz without hold time.

The predictions were made by using Equations (4) and (8) with C = 2.9678E-11 m/sec and m = 2.65. The value for the $(da/dN)_C$ term was set to those experimental data points for f = 10Hz. It is seen that the correlation between Equation (8) and the trapezoidal load test data is quite good.

It is also shown in Figure 4 that Equation (8) correlates with those triangular load test data in the time dependent region (f ≤ 0.02Hz, or total time ≥ 50 sec.) but fails to predict the crack growth rates in the mixed region (0.02 < f < 10Hz). For this group of data, a better correlation was obtained by using the latest version of the Saxena Equation,[9] i.e.,

$$\frac{da}{dN} = \left(\frac{da}{dN}\right)_c + C_4 \cdot \Delta K^{\alpha} \cdot [1/\sqrt{f} - 1/\sqrt{f_0}] \qquad (9)$$

where $f_0$ is the characteristic frequency, which separates the cycle dependent and the mixed regions. For those data sets in Figure 4, the value for $f_0$ was assumed to be 10Hz. Using a procedure given by Saxena,[12] it was determined that $C_4$= 1.075E-10, α = 2.35.

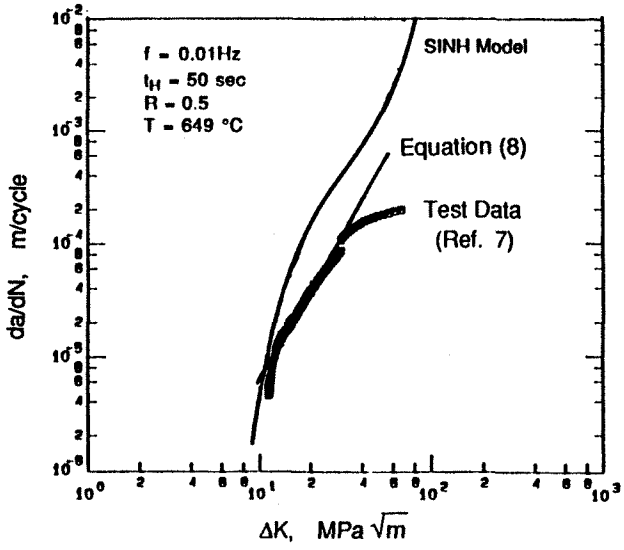


Fig 5 Comparison of predicted and test results for the INCO 718 alloy at R = 0.5

The example case shown in Figure 5 involves all three loading variables, $t_H$, $t_r$, and R (as compared to those data sets shown in Figure 4 of which the crack growth rates were functions of $t_H$ and R, or f and R). The test condition for this data set was: R = 0.5, f = 0.01Hz (i.e., $t_r$ = 50 sec.), $t_H$ = 50 sec., $K_{max}$ = 20-140 MPa $\sqrt{m}$ ($\Delta K$ = 10-70 MPa $\sqrt{m}$). It is evident that a perfect match was obtained (up to $\Delta K$ = 35 MPa $\sqrt{m}$). It is also clear that the present approach (i.e., Equation (8) is superior to the other crack growth models. A comparison with the SINH model,[13] a model that is widely used by the engine industry, is shown in Figure 5.

In conclusion, it can be stated that the crack growth behavior of a stress cycle having a trapezoidal wave form can be predicted by using the combination of conventional high frequency da/dN data, sustained load data (da/dt), and Equation (8). For those stress cycles having a triangular wave form, test data for a specific frequency in question may be required. Otherwise, a set of test data containing several frequencies is needed for developing those empirical constants in the Saxena equation. It should be noted that Equation (9) is basically an empirical function for curve fitting and data interpolation, it is not a scientific rule that dictates the frequency effect on crack growth behavior. Therefore, although not essential, it is desirable to have an all around method that can describe the da/dN behavior in the mixed region.

In summary, whenever the effect of load interaction is absent, the total crack growth rate for a loading block containing both triangular and trapezoidal stress cycles will be

$$\left(\frac{da}{dN}\right)_{Total} = \sum_i \left(\frac{da}{dN}\right)_i \qquad (10)$$

where i denotes the ith loading step in the entire group of loads under consideration. The amount of da for each loading step is determined by using Equation (8), or (9).

## LOAD/ENVIRONMENT INTERACTION

An aircraft load spectrum consists of numerous stress cycles. For simplicity, it is assumed that the shape of an individual stress cycle will be either sinusoidal (triangular), or trapezoidal. A loading block may contain both types of stress cycles. Some typical combinations (in magnitude and shape) are shown in Figure 1. Crack growth rates can be significantly different in between any two types of these stress profiles. Load interaction is believed to be the source affecting the crack growth rate behavior. Several possible mechanisms are discussed in the following subsections.

### The Basic Concept of Load Interaction

When a crack is subjected to a cyclic stress, due to the high stress concentration at the tip of a sharp crack, even though the applied stress level might have been very low, the bulk of material in front of the crack would have undergone plastic yielding. According to Irwin,[14] the size of a crack tip plastic zone can be expressed as

$$r_p = \frac{\beta}{\pi} \cdot (K_{max}/F_{ty})^2 \qquad (11)$$

Here $F_{ty}$ is the material tensile yield strength, ß accounts for the degree of plastic constraint at the crack tip. For example, ß = 1 for a through the thickness crack in a thin sheet because the stress state at the crack tip is plane stress. The value of ß decreases to 1/3 as the stress state changes from plane stress to plane strain. Upon unloading, there are residual stresses remaining on the crack plane; these residual stresses interact with those singular stress fields of the subsequent stress cycles. The actual driving force for crack growth will be an effective stress field which accounts for the contributions of the applied stress and the residual stresses.

There are many ways to determine the instantaneous effective stress field (resulting from mechanical load interaction) at room temperature. The analytic models of References (15)-(17) are representative of those being used in the aircraft/aerospace industry today. Discussions on how to handle special situations such as crack growth in a stress field containing pre-existing residual stresses are available in the open literature.[18]-[21] This paper will not discuss any of these models and techniques; however, in the following paragraphs a hypothetical stress profile (depicted in Figure 6) is used to illustrate the load interaction phenomena.

During crack propagation under variable amplitude loading, there is a crack tip plastic zone associated with each stress cycle. However, Equation (11) is for a stationary crack, not a growing crack. In a given step, the plastic zone is calculated based on the current crack length and the load applied to it, and is placed in front of that crack length as shown in Figure 6. In this manner, there will be no load interaction if the elastic-plastic boundary of the current plastic zone exceeds the largest elastic-

plastic boundary of the preceding plastic zones. In other words, load interaction exists as long as the plastic zone for the current stress cycle is within the elastic-plastic boundary remaining from any of the preceding stress cycles.

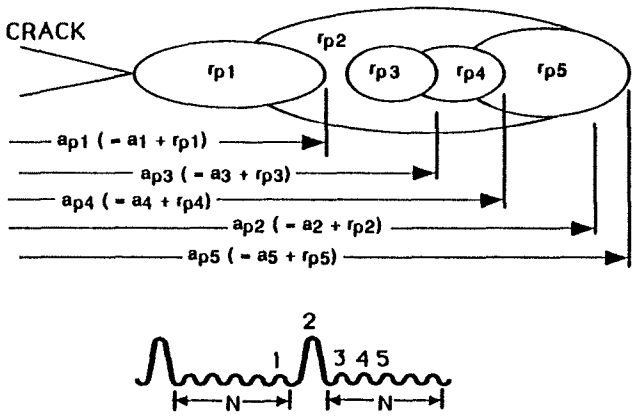


Fig. 6 Schematic definition of load interation zones

Consider a stress level $S_1$, which is being applied to a crack length $a_1$, this action will create a plastic zone $r_{p1}$ in front of the crack as schematically shown in Figure 6. The elastic-plastic boundary for this stage in the crack growth history will be $a_{p1}$ ( = $a_1$ + $r_{p1}$). Meanwhile, the crack will grow from $a_1$ to $a_2$. The stress event that follows, i.e., $S_2$, will create another plastic zone $r_{p2}$ in front of $a_2$, so that the elastic-plastic boundary will become $a_{p2}$ ( = $a_2$ + $r_{p2}$). Since $a_{p2} > a_{p1}$, there is no load interaction while the crack is extending from $a_2$ to $a_3$. In the following three steps, both $a_{p3}$ and $a_{p4}$ are smaller than $a_{p2}$ but $a_{p5}$ finally travels through the previous elastic-plastic boundary, i.e., $a_{p5} > a_{p2}$. Therefore, load interactions exist in those two steps that are involved with $a_{p3}$ and $a_{p4}$. Crack growth rates will be effected by the residual stress field associated with $a_{p2}$ while the crack is propagating from $a_3$ to $a_4$, and from $a_4$ to $a_5$. By definition, there is no load interaction between $a_{p5}$ and $a_{p2}$ because $a_{p5} > a_{p2}$. Thus, the growth of $a_5$ (to $a_6$, not shown) will be solely due to $S_5$.

Crack Tip Deformation Mechanisms at High Temperature

The preceding section has presented a crack growth accumulation technique that is typical of those used in today's room temperature crack growth life prediction methodology. It has shown that this approach is also applicable to crack growth at high temperatures, whether a test is run under a uniform temperature (isothermal), or having the temperatures change along with the applied stresses.[1] The crack tip plastic zone sizes can be computed by using Equation (11) with $F_{ty}$ being the material tensile yield strength at temperature.

The dwell time in a trapezoidal stress cycle promotes creep deformation at the crack tip. The $F_{ty}$ term in Equation (11) may be considered as an effective yield stress required to achieve a 0.2 percent strain in a creep test. The effective yield stress to room temperature tensile yield strength ratio can be plotted against the Larsen-Miller parameter, which takes into account the combined effect of temperature and time at load. An actual example (for the INCO 718 alloy) is given in Figure 7.

Other than the plastic zone, hold times at load can cause two other types of deformation zones at the crack tip, i.e., the creep zone, and the environment

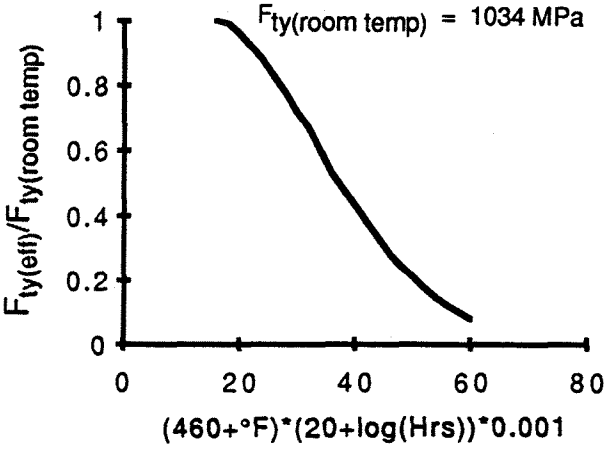


Fig. 7 Effective yield strength for the INCO 718 alloy

affected zone (EAZ). All three types of crack tip deformation zones can coexist at a given time. Each of them has a unique way in controlling the crack growth rates for the current and the subsequent cycles. Thus, the plastic zone is the source for altering the crack tip stress field during crack propagation. The size of a creep zone indicates the relative degree of creep deformation. It can be used as a guide to determine whether crack growth will be controlled by K, or $C_t$, or $C^*$.

If a material is sensitive to environment, e.g., the INCO 718 alloy, the material near the crack tip would be severely damaged by the environment. In the case of high temperature crack growth testing, oxidation due to penetration of hot air into a localized crack tip region is considered the primary source for creating the "damaged zone," which is being called the environment affected zone (EAZ). The "damaged" material inside the EAZ no longer represents the original bulk material and exhibits

accelerated crack growth rates (as compared to its baseline behavior).

The methods for determining the creep zone and the EAZ are discussed in the following paragraphs.

The Creep Zone:

For a stationary crack, the size of a creep zone is given by Riedel and Rice,[22] as

$$r_{cr} = \frac{K}{2\pi} \cdot (EAt)^{2/(n-1)} \cdot F_{cr} \qquad (12)$$

where K is the stress intensity level, E is the material elastic modulus. The values of A and n are, respectively, the constant and the stress exponent of Equation (1). The term $F_{cr}$ is a polar function centered at the crack tip.[22] Its value depends on n, and other plasticity coefficients.[23],[24] A set of the $F_{cr}$ values (computed for a Poisson ratio of 0.3) is presented in Figure 8.

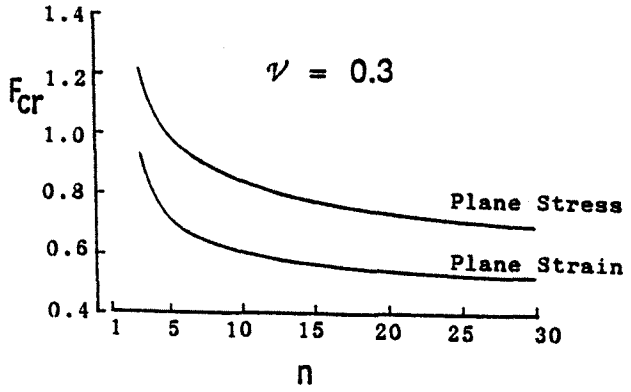


Fig. 8 Creep zone size dimensionless coefficient $F_{cr}$

The Environment Affected Zone:

At the present time, experimental testing is the only means for determining the EAZ size and the crack growth rate behavior inside the EAZ. Consider a loading profile which consists of one trapezoidal stress cycle and many triangular (or sinusoidal) stress cycles. The test was conducted in such a way that a constant K level was maintained at each stress cycle (see the sketch shown in Figure 9). The crack growth rate for each of the triangular stress cycles can be plotted as a function of crack lengths. A typical example, taken from Reference 25, is shown in Figure 9. For convenience, the crack length immediately following the sustained load cycle is being set to 0. It appears that this group of data points is divided into two parts. Each part can be approximated by a straight line. The first part characterizes the crack growth behavior inside the EAZ where the crack growth rate is initially higher than normal, because the material has been damaged by the high temperature environment. It gradually decreases to a

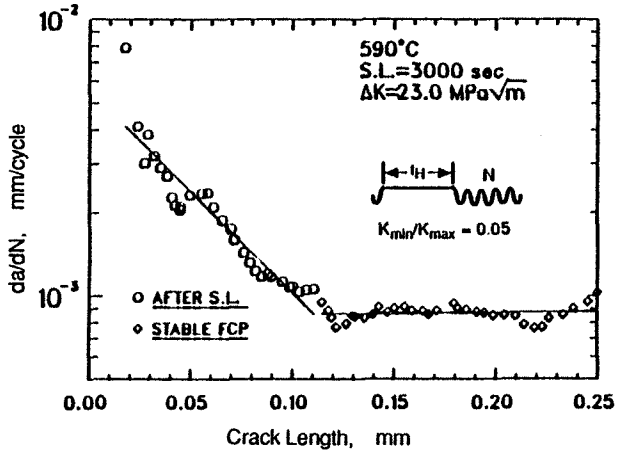


Fig. 9 Measured da/dN after a sustained load cycle

level that is otherwise normal for an undamaged material. The horizontal line implies that the crack had traveled through the EAZ and resumes a stable crack growth behavior. Therefore, the intersection of these two lines determines the size of the EAZ.

There are many ways to formulate an empirical equation for the EAZ. In dealing with crack growth of aluminum in salt water (at room temperature), Kim and Manning,[26] hypothesized that EAZ (which is attributed to hydrogen penetration) is in proportion to the crack tip plastic zone size (which is a function of the applied K), and D (the diffusion coefficient of hydrogen in aluminum), and $t_H$. However, based on high temperature crack growth data of the INCO 718 alloy, Chang,[27] concluded that EAZ (attributed to oxidation) was a function of hold time and temperature, independent of K. Thus, Chang further postulated that the EAZ's could be fitted by an empirical equation of the form:

$$r_e = \lambda \cdot (t_H)^n \cdot EXP(-Q/RT) \qquad (13)$$

Here, EAZ is denoted as $r_e$, T is the absolute temperature (in °K), Q is the activation energy, R is the gas constant (= 8.314 J/°K), $\lambda$ and n are empirical constants.

Chang's data are plotted in Figure 10. Using Equation (13) with Q = 60000 cal/mole (= 251400 J) for nickel base super alloy, the empirical constants $\lambda$ and n can be determined by fitting a regression line through all the experimental data points. In this case, $\lambda$ = 7.55E10 mm/sec and n = 1.0.

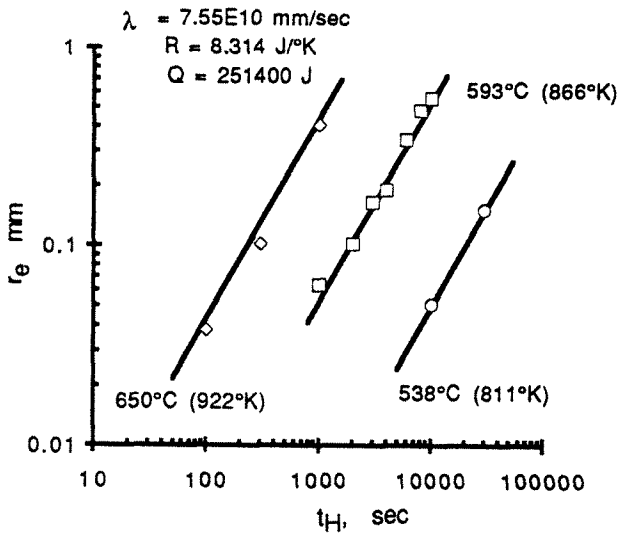


Fig. 10 EAZ sizes for the INCO 718 alloy

Damage Accumulation Modeling

An aircraft flight spectrum consists of various types of load segments. It is a composite of all (but not limited to) those loading profiles shown in Figure 1. For simplicity, all these loading segments can be regarded as if they were the same except that each load cycle (in a given profile) may have a different magnitude, frequency, or hold time. On the basis of all the information gathered in the previous review,[1] it is reasonable to assume that the general scheme of the current room temperature crack growth accumulation monitoring routine (depicted in Figure 6) can be adapted for computing spectrum crack growth history at high temperature. An extension of this methodology requires the calculation of all three types of crack tip deformation zones at each loading step, and implementing a complicated "book keeping" routine to track all the loading events, the size of each crack tip deformation zone (created by each loading step) and the relative position of the crack tip inside these zones, and the computed damages.

Taking the INCO 718 alloy for example, the sizes for all three crack tip deformation zones at 650 °C (1200 °F) corresponding to an applied K level of 25 MPa$\sqrt{m}$ have been computed, using Equations (11)-(13). The coefficients in Equation (12), for the creep zones at 650 °C are: A =1.83e-47 $(MPa)^{-n/hr}$, n = 15.8, E = 1.66e+05 MPa. The effective $F_{ty}$ values are computed by using Figure 7, and setting the monotonic $F_{ty}$ (i.e., at $t_H$ = 0) at 848 MPa. The EAZ sizes are directly obtained from Figure 10. As shown in Figure 11, the plastic zone is significantly larger than its creep zone counterpart at any given time. Therefore it can be said that the "small scale creep" condition is being maintained. The driving force for crack extension will be K, not $C_t$ or $C^*$. Crack growth of this material/temperature system will be primarily dominated by $r_p$ and EAZ. The "book keeping" routine for monitoring cumulative damages eventually can be simplified by ignoring the creep zone. The step by step crack growth increments can be determined following the scenario of Figure 6. In each step, the current sizes of $r_p$ and EAZ are computed using Equations (11) and (13), an effective stress intensity factor is computed by implementing one of the crack growth analysis models mentioned earlier. The crack growth rate for a given loading step will then be determined by using Equations (8), (9) and (10) in conjunction with the required da/dN and da/dt data. However, the accelerated da/dN data for "damaged material" should be used as long as the crack is inside an EAZ.

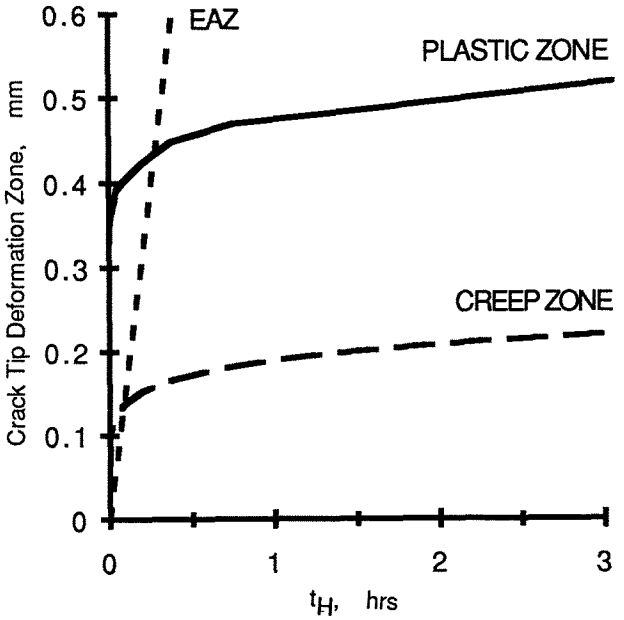


Fig. 11 Crack tip deformation zone sizes for the INCO 718 at 650 °C

CONCLUDING REMARKS

An assessment of high temperature crack growth analysis methodology has been conducted. It can be concluded that as long as load/environment interactions are absent, Equations (8), (9) and (10) can adequately predict crack growth in the cycle dependent and the time dependent regime. An attempt was made to enhance the existing load interaction model (for room temperature) to handle high temperature crack growth under variable amplitude and variable wave form loadings involving all three types of crack tip deformation modes (i.e., plasticity, creep, and environment induced damage).

This paper only concerns the crack growth mechanisms in the environment sensitive alloys. Some alloy that is normally susceptible to environment may become susceptible to creep at higher temperatures. When an alloy is somewhat susceptible to creep (even though crack extension is still controlled by K), crack growth behavior inside an EAZ may not be the same as those shown in Figure 9. Specifically, the crack growth rates may be retarded instead of accelerated (see Reference 28 for high temperature crack growth testing of the IN100 alloy). With regard to this, a clearly defined criterion for the transition of crack tip deformation modes is needed. Experimental investigation on identifying post sustained load crack growth behavior under various loading conditions and material/temperature systems such as titanium aluminides and metal matrix composites deserves special attention. Crack growth data of this kind are needed for developing methodologies to model load/temperature/time interactions between a dwell cycle and the sinusoidal load cycles.

Due to lack of verification test data, of which the loads spectrum contains various mixtures of temperatures and hold time, it is impossible to assess the accuracy of the proposed method. In any event, there is sufficient information gathered here to formulate a generic crack growth predictive methodology for aircraft structural life prediction.

## REFERENCES


1. Liu, A. F., "Element of Fracture Mechanics in Elevated Temperature Crack Growth," AIAA Paper No. 90-0928, presented at the AIAA/ASME/ASCE/AHS/ASC 31st Structures, Structural Dynamics and Materials Conference, Long Beach, CA, April 2-4, 1990, in Collection of Technical Papers, Part 2, pp. 981-994.

2. Saxena, A., in Fracture Mechanics: Microstructure and Micromechanisms, ASM International, 1989.

3. Riedel, H., in Flow and Fracture at Elevated Temperatures, American Society for Metals, 1983, pp. 149-177.

4. Ghonem, H., Nicholas, T. and Pineau, "Analysis of Elevated Temperature Fatigue Crack Growth Mechanisms in Alloy 718," presented at the ASME Winter Annual Meeting, 1991.

5. Shih, T. T. and Clarke, G. A., in Fracture Mechanics, ASTM STP 677, 1979, pp. 125-143.

6. Nicholas, T. and Ashbaugh, N. E., in Fracture Mechanics: Nineteenth Symposium, ASTM STP 969, 1988, pp. 800-817.

7. Haritos, G. K., Nicholas, T. and Painter, G. O., in Fracture Mechanics: Eighteenth Symposium, ASTM STP 945, 1988, pp. 206-220.

8. Nicholas, T. and Weerasooriya, T., in Fracture Mechanics: Seventeenth Volume, ASTM STP 905, 1986, pp. 155-168.

9. Saxena, A. and Basani, in Fracture: Interac-tions of Microstructure. Mechanisms and Mechanics, Proceedings of the Symposium, 113th AIME Annual Meeting, Los Angeles, California, February, 27-29, 1984, pp. 357-383.

10. Wei, R. P. and Landes, J. L., Materials Research and Standards, TMRSA, Vol. 9, 1969, pp. 25-28.

11. Liu, A. F., Journal of Aircraft, Vol. 23, 1986, pp. 333-339.

12. Saxena, A., Fatigue of Engineering Materials and Structures, Vol. 3, 1981, pp. 247-255.

13. Schwartz, B. J. and Annis, C. G., Jr., Engineering Fracture Mechanics, Vol. 18, No. 4, 1983, pp. 815-836.

14. Irwin, G. R., "Plastic Zone Near a Crack and Fracture Toughness," Proceedings of the Seventh Sagamore Ordinance Material Research Conference, Report No. METE 661-611/F, Syracuse University Research Institute, 1960, p. IV-63.

15. Willenborg, J. D., Engle, R. M. and Wood, H. A., "A Crack Growth Retardation Model Using an Effective Stress Concept," AFFDL-TM-71-1-FBR, 1971.

16. Saff, C. R., in Damage Tolerance of Metallic Structures, ASTM STP 842, 1984, pp. 36-49.

17. Newman, J. C., Jr., "FASTRAN II - A Fatigue Crack Growth Structural Analysis Program," NASA TM 104159, February, 1992.

18. Nelson, D. V., in Residual Stress Effects in Fatigue, ASTM STP 776, 1982, pp. 172-194.

19. Liu, A. F., Journal of Engineering Materials and Technology, Trans. ASME, Series H, Vol. 104, 1982, pp. 153-154.

20. Rudd, J. L., Hsu, T. M. and Aberson, J. A., in Numerical Methods in Fracture Mechanics, Proceeding of the First International Conference, Univ. College of Swansea, West Glamorgan, U. K., Jan. 9-13, 1978.

21. Cathey, W. H. and Grandt, A. F., Jr., Journal of Engineering Materials and Technology, Trans. ASME, Series H, Vol. 102, 1980, pp. 85-91.

22. Riedel, H. and Rice, J. R., in Fracture Mechanics, Proceedings of the Twelth National Symposium on Fracture Mechanics, ASTM STP 700, 1980, pp. 112-130.

23. Hutchinson, J. W., Journal of Mechanics and Physics of Solids, Vol. 16, 1968, pp. 337-347.

24. Shih, C. F., "Table of Hutchinson-Rice-Rosengren Singular Field Quantities," Report No. MRL E-147, Brown University, Providence, RI, June, 1983.

25. Chang, K. M., in Effects of Load and Thermal Histories on Mechanical Behavior of Materials, The Metallurgical Society, Inc., 1987, pp. 13-26.

26. Kim, Y. H. and Manning, S. D., in Fracture Mechanics, Fourteenth Symposium, Vol. I: Theory and Analysis, ASTM STP 791, 1983, pp. I-446-I-462.

27. Chang, K. M., Material Research Symposium Proceedings, Vol. 125, Material Research Society, 1988, pp. 243-252.

28. Larsen, J. M. and Nicholas, T., in Fracture Mechanics, Fourteenth Symposium, Vol. II: Testing and Applications, ASTM STP 791, 1983, pp. II-536-II-552.